

Telecom-Band Entanglement Generation for Chipscale Quantum Processing

Kim Fook Lee, and Prem Kumar,^{1,*} Jay E. Sharping, Mark A. Foster,
and Alexander L. Gaeta,² and Amy C. Turner, and Michal Lipson³

¹*Center for Photonic Communication and Computing, EECS Department,
Northwestern University, 2145 Sheridan Road, Evanston, IL, 60208, USA*

²*School of Electrical and Computer Engineering,
Cornell University, Ithaca, NY 14853*

³*School of Applied and Engineering Physics,
Cornell University, Ithaca, NY 14853*

(Dated: October 29, 2006)

Abstract

We demonstrate polarization-entanglement for non-degenerate and degenerate photon-pairs generated through Kerr-nonlinearity in a nano-scale silicon-on-insulator (SOI) waveguide. We use a compact counter propagating configuration to create two-photon polarization-entangled state, $|H\rangle|H\rangle + |V\rangle|V\rangle$. We observe two-photon interference with visibility $> 91\%$ and $> 80\%$ for non-degenerate and degenerate photon-pairs, respectively. The experimental structure can be implemented on optical chips as an integrated source of entangled photons for future quantum computer and communication applications.

Four-photon scattering (FPS) in a dispersion shifted fiber has proven to be an essential nonlinear process for providing both non-degenerate and degenerate telecom-band photon-pairs in many proof of principle experiments [1, 2, 3, 4, 5, 6, 7]. Briefly, two pump photons at frequency ω_p scatter through the four-photon scattering to create signal(ω_s) and idler (ω_i) photons, such that $2\omega_p = \omega_s + \omega_i$ and $2k_p = k_s + k_i$. This process is always referred to non-degenerate FPS. While in the reverse degenerate FPS, one pump photon at signal frequency (ω_s) and one pump photon at idler frequency (ω_i) will annihilate together to create two degenerate photon-pair at frequency (ω_p). For practical quantum communication, non-degenerate entangled photon-pairs are desirable for entanglement distribution in a wavelength-division multiplexing (WDM) environment [8, 9], and enabling parallel multi-users access. While the degenerate entangled photon-pairs are suitable for quantum computers because quantum logic gates are essentially complicated interferometers which usually require quantum interference of two indistinguishable photons such as Hong-Ou-Mandel interference [10].

The advanced of nano-technology in fabrication [11] and atto-second light source in light manipulation [12] motivate the possibility of implementing practical quantum information and schemes in an optical chip. Silicon photonics is a most recent promising technology for providing a integrated optics platform [13]. Waveguide confinement in SOI waveguides can yield net anomalous group-velocity dispersion and enable four-wave mixing process in classical domain [14]. Prior to this present work, we have observed the generation of correlated photon-pairs through the FPS in the SOI waveguide [15]. However, nonclassical correlation and polarization-entanglement of the generated photon-pairs have not been investigated.

In this work, we extend our study to demonstrate nonclassical nature of two-photon coincidences of the generated signal-idler photon-pairs in the SOI waveguide. For this purpose, we use the similar experiment setup as shown in ref[[15]]. Briefly, we launch a linearly polarized pump light into SOI waveguide, then the generated signal-idler photon-pair are spectrally filtered out through their individual WDM filters and hence provides signal and idler quantum channels. In order to prove that the photon-pairs exhibit nonclassical correlation, we need to violate classical inequality which is valid for two classical light sources, as given by [16],

$$R_c^{s,i} - R_{ac}^{s,i} - 2(R_c^{s/2} - R_{ac}^{s/2} + R_c^{i/2} - R_{ac}^{i/2}) \leq 0, \quad (1)$$

where $R_c^{s,i}$ and $R_{ac}^{s,i}$ are the coincidence and calculated accidental coincidence count rates for the signal and idler channels. The lights in signal and idler channels are assumed to be the two classical light sources. $R_c^{s/2}$ and $R_{ac}^{s/2}$ ($R_c^{i/2}$ and $R_{ac}^{i/2}$) are the coincidence and calculated accidental coincidence count rates measured by passing the signal (idler) channel through a 50/50 beamsplitter, respectively. For nonclassically correlated signal-idler photon pairs, the term $R_c^{s,i} - R_{ac}^{s,i}$ in Eq. 1 is the true two-photon coincidences which will be proportional to photon-pair production rate. While the term $(R_c^{s/2} - R_{ac}^{s/2} + R_c^{i/2} - R_{ac}^{i/2})$ in Eq. 1 vanishes because the probability for observing a photon-pair in either signal or idler channels is zero. We measure the inequality as a function of average pump power in the waveguide as shown in Fig. 1. We observe larger violation of the inequality as we increase the average pump power which corresponds to the increase of photon-pair production rate. Our experimental result confirms that the signal-idler photon-pair generated through FPS in the waveguide is indeed nonclassically correlated. From the same experimental data, we plot coincidences to accidentals ratio (CAR) and obtain the peak ratio of $\simeq 30$. At the peak ratio where the average pump power is about $90\mu W$, the Eq. 1 yields $(67 \pm 10) \times 10^{-7}$ which provides the violation over 6 standard deviations. One should adopt CAR as the best estimate for the purity of the correlated photon-pairs before the source can be used for many practical quantum processing, where the accidental-coincidence counts contributed from background photons are inevitable.

In the second experiment, we study the generation of polarization-entangled photon-pairs through non-degenerate and degenerate FPS in a SOI waveguide. Since the FPS process only occurs in the transverse electric (TE) mode of SOI waveguide, we need to modify the counter-propagating scheme (CPS) [17, 18, 19] so that the created two-photon polarization-entangled state propagates in the direction opposite to the incoming input pump field. We observe two-photon interference with visibility $> 91\%$ and 80% for non-degenerate and degenerate cases, respectively. These results are promising for realization of chip, and future quantum computer and communication applications.

As shown in Fig. 2(a), the pump is a mode-locked pulse train with pulse duration $\simeq 5$ ps and repetition rate of 50.3 MHz. The pump is initially obtained from a femtosecond fiber laser by using a WDM filter with 1 nm full-width at half-maximum (FWHM) passband. The pump central wavelength is at 1555.9 nm. To achieve the required power, the pump pulses are further amplified by an erbium-doped fiber amplifier (EDFA). The amplified

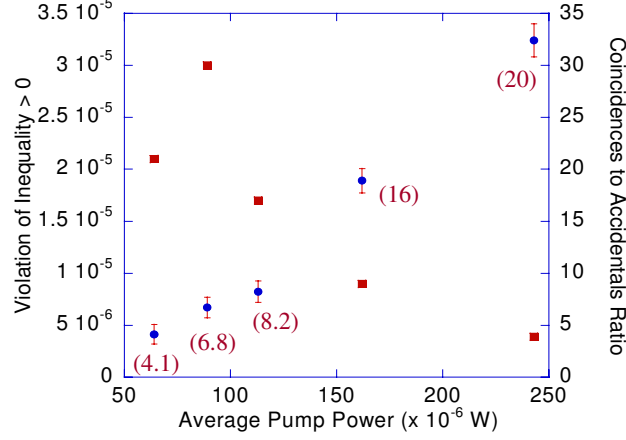


FIG. 1: Measurement on the violation of classical inequality in Eq. 1 (circle) and coincidences to accidentals ratio (square) for the generated signal-idler photon pairs in the SOI waveguide. The number in the parenthesis indicates the order of violation over standard deviations of measurement uncertainty.

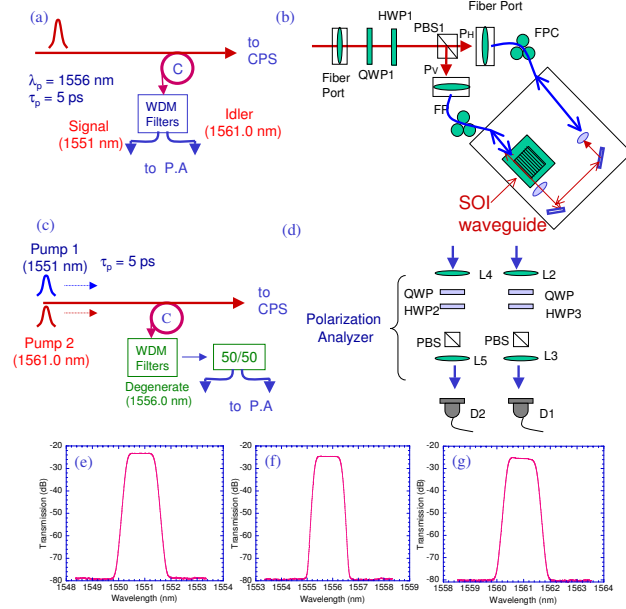


FIG. 2: A schematic of the experimental setup. (a) The input pump field for nondegenerate FPS. (b). The CPS with SOI waveguide. (c). The two pump fields for degenerate FPS. (d). Polarization analyzers for signal and idler photons. FP, fiber-port; LP, linear polarizer; L2, L3, L4, L5, fiber-to-free space collimators; PBS, polarization beamsplitter; HWP, QWP, half- and quarter-wave plates; FPC, fiber polarization controller. The WDM filter shape for (e) the signal, (f) the pump and (g) the idler.

spontaneous emission (ASE) from the EDFA is suppressed by passing the pump through the two cascaded WDM filters. The pump power goes through a fiber circulator(C)) to the CPS. The configuration setup for the SOI waveguide is shown as a small box in Fig. 2(b). The waveguide is a 9.33-mm long and its cross section is 600 nm x 300 nm. It has built-in an inverse taper at both ends. We couple the light into the waveguide using a lensed fiber. The polarization of the input field has to be aligned parallel to the TE mode of the waveguide. We then use a 3 mm focal-length aspheric lens to collect the output light from the waveguide. A regular free-space to fiber collimator is used to couple the light back into fiber. Before the CPS is used to create two-photon polarization-entangled state, we want to make sure all birefringence sensitive devices including SOI waveguide and polarization analyzers are properly aligned and compensated. Briefly, we use half wave-plate (HWP1) and quarter wave-plate (QWP1)in the CPS to adjust the input pump field so that it is vertically polarized at the PBS1. This pump will travel in the counter-clockwise direction of the CPS. Fiber polarization controller (FPC1) is used to transform the pump field into the TE mode of the waveguide. Then, the polarization of the generated signal and idler photons together with the pump photon in the counter-clockwise direction in the CPS are transformed by the FPC2 to horizontal polarization. They transmit through the PBS1 in the direction opposite to the incoming pump field and back to the circulator. The signal and idler photons are filtered out and sent to the polarization analyzers (PA). A set of QWP and HWP in the PA is used to compensate the polarization birefringence effects experienced by the signal and idler photons since they traveled from the PBS1, so that they are retained to horizontal polarization before the PBS. The angle settings of HWP2 and HWP3 in signal and idler channels are then referred to the detection polarization angles $\theta_1 = 0$ and $\theta_2 = 0$. Now, if the HWP1 is rotated to 45° , the input pump field is transformed to horizontally polarized field. This pump field propagates in the clockwise direction of the CPS. With the same polarization transformation provided by the FPC2 and FPC1, the generated signal and idler photons in the clockwise direction are transformed to vertical polarization and reflected at the PBS1 to the opposite direction of incoming pump field. In the backward direction, one should realize that the HWP1 at 45° will again transform the vertical polarization state of the reflected lights to horizontal polarization state. The independent optimizations of the electric field polarization alignments in counter-clockwise and clockwise directions of this CPS and SOI waveguide are essential due to the fact that the FPS only occurs in TE mode.

We now rotate the HWP1 to 22.5° so that the input pump field at the PBS1 is now split into two equally powered, orthogonally polarized components P_H and P_V . For low four-photon scattering efficiencies, where the probability for each pump pulse to scatter more than one pair is low, the clockwise and counter-clockwise pump pulses scatter signal/idler photon-pairs with probability amplitudes $|H_i\rangle|H_s\rangle$ and $|V_i\rangle|V_s\rangle$, respectively. After propagating through the SOI waveguide, these two amplitudes of the photon-pair are then coherently superimposed through the same PBS1. This common-path polarization interferometer has good stability for keeping zero relative phase between horizontally and vertically polarized pumps, and hence is capable of creating polarization-entanglement of the form $|H_i\rangle|H_s\rangle + |V_i\rangle|V_s\rangle$ at the input port of the PBS1. Since the two-photon polarization-entangled state propagates in the opposite direction of input pump field, one should realize that the HWP1 at 22.5° again rotates the two-photon state to 45° basis. This backward action can be compensated at the signal and idler channels by adding the initial angle settings of HWP2 and HWP3 by the amount of 22.5° . Note that one could keep the initial angle settings of HWP2 and HWP3 and account the backward action of HWP1 as projecting the signal and idler photons to 45° prior to coincidence detection. Since the correlation function of the entangled state $|H_i\rangle|H_s\rangle + |V_i\rangle|V_s\rangle$ is $\cos^2(\theta_1 - \theta_2)$, either option as mentioned above gives maximum coincidence counts. To reliably detect the scattered photon-pairs, an isolation between the pump and signal/idler photons in excess of 100 dB is required. We achieve this by using two cascaded WDM filters with FWHM of about 1 nm in the signal and idler channels, which provide total pump isolation greater than 110 dB. The selected signal and idler wavelengths are 1550.95 nm and 1561.0 nm, respectively, corresponding to $\simeq 5.0$ nm detuning from the pump's central wavelength. The photon-counting modules consist of InGaAs/InP avalanche photodiodes operated at a rate of 780 kHz, which is downcounted by 1/64 from the original pump pulses. The total detection efficiencies for the signal and idler photons are about 0.7% and 0.8%, respectively.

We measure two-photon interference to justify the purity of the entangled photon-pairs generated by SOI waveguide. The average power for each pump in the waveguide is $96\mu W$ after including the 80% coupling efficiency of the fiber-port, 80% transmission of the FPC1 and also 10% coupling efficiency from the tapered fiber to waveguide. We fix θ_1 , and vary θ_2 , and record single counts for both signal and idler channels as well as coincidence counts between the two channels for each value of θ_2 . We observe TPI with visibility $> 91\%$ as

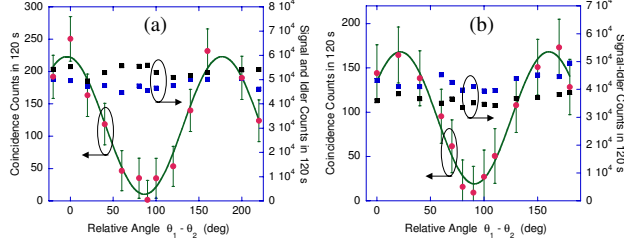


FIG. 3: The measured two-photon interference for (a) non-degenerate and (b) degenerate polarization entangled photon-pairs with visibility $> 91\%$ and $> 80\%$, respectively.

shown in Fig. 3(a), without subtraction of accidental-coincidences. The fitting function used in the figure is $\cos^2(\theta_1 - \theta_2)$. The photon-pair production rate is about 0.08. The visibility of TPI is in agreement with our current and previous measurements [15] on CAR of 25-30 for the correlated non-degenerate photon-pairs generated in the same waveguide.

We further study the purity of degenerate entangled photon-pair with the CPS and SOI waveguide. For this purpose, we use the similar experimental scheme [6] to prepare two input pump fields. Briefly, we spectrally filter out the desired pump central wavelengths at $\omega_{p1} = 1550.95$ nm and $\omega_{p2} = 1560.01$ nm by using a double-grating filter (DGF) with FWHM of 0.8 nm. These two pumps are combined together and then amplified by using EDFA. After the EDFA, the two input pump fields are further filtered out by a second DGF. We then combine them in a WDM by using the following configuration as $(P + R \rightarrow C)$. We also make sure the two independent input pump fields to be overlapped in time and equal power, so that the phase matching condition of the reverse degenerate FPS is optimized in the waveguide. The degenerate two-photon polarization-entangled state is created by the similar manner in the CPS as described in the non-degenerate case. The degenerate photon-pairs at wavelength of 1555.9 nm is filtered out by using two cascaded WDM filters. In order to bring the degenerate photon-pairs into two spatially separated detectors, we need to use a 50/50 fiber beamsplitter after the WDM filters as shown in Fig. 2(c). By doing this, we post-select the case where the photon-pair splits leading to coincidence detection. In other words, after the 50/50 beamsplitter, we use coincidence measurement to post-project the state $|H\rangle|H\rangle + |V\rangle|V\rangle$. The average power for each pump used in this scheme is $288\mu W$ which corresponds to photon-pair production rate of 0.12. We measure two-photon interference and observe TPI with visibility $> 80\%$ as shown in Fig. 3(b).

All the above measurements are made without subtracting the accidental coincidence

counts. Even though literature [20] predicts that spontaneous Raman scattering process (RS) in the TE mode of the waveguide could exhibit a narrow peak with a FWHM of 0.8nm located at about 100nm away from the pump, but so far no photon-counting measurement is conducted to measure how the RS spreads from the narrow peak to the pump. We believe that the Raman scattering photons prevent this entangled source to achieve TPI with unit visibility. Since it is a chip-scale waveguide, it can be easily cooled to suppress RS photons. And also, the detection efficiencies in the experiments are low due to the coupling loss, which could be one of the main reason in degradation of the two-photon entanglement. Degenerate photon-pairs exhibit lower TPI visibility compared with non-degenerate photon-pairs because we use higher average power for two pump fields through the EDFA which could create in-band ASE noise photons to the detection.

In conclusion, we have demonstrated the generation of polarization-entanglement for non-degenerate and degenerate photon-pairs in a SOI waveguide. We believe the nano-scale silicon based entanglement source will lead to realistic implementations of quantum communication and computing protocols. This work is supported in part by the NSF under Grant No. EMT- 0523975.

This work is supported in part by the NSF under Grant No. EMT- 0523975.

* kflee@ece.northwestern.edu

- [1] J. E. Sharping, M. Fiorentino, and P. Kumar, Opt. Lett. **26**, 367 (2001).
- [2] M. Fiorentino, P. L Voss, J. E. Sharping, and P. Kumar, Photon. Technol. Lett. **14**, 983 (2002).
- [3] X. Li, P. L Voss, J. E. Sharping, and P. Kumar, Phys. Rev. Lett. **94**, 053601 (2005).
- [4] X. Li, J. Chen, P. L Voss, J. E. Sharping, and P. Kumar, Opt. Express **12**, 3737 (2004).
- [5] K. F. Lee, J. Chen, C. Liang, X. Li, P. L Voss, and P. Kumar, Opt. Lett. **31**, 1905 (2006).
- [6] J. Chen, K. F. Lee, C. Liang, and P. Kumar, Opt. Lett. **31**, 2798 (2006).
- [7] C. Liang, K. F. Lee, T. Levin, J. Chen, and P. Kumar, Opt. Express **14**, 6936 (2006).
- [8] C. Liang, K. F. Lee, J. Chen, and P. Kumar, Optical Fiber Communications Conference (OFC'2006), Anaheim Convention Center, Anaheim, CA, March 5-10 **See paper 06-P-2219-OFC/NFOEC**, postdeadline paper (2006).

- [9] X. Li, P. L Voss, J. Chen, J. E. Sharping, and P. Kumar, Opt. Lett. **30**, 1201 (2005).
- [10] C. K. Hong, Z. Y. Ou and L. Mandel, Phys. Rev. Lett. **59**, 2044 (1987).
- [11] W. A. Goddard III, D. W. Brenner, S. E. Lyshevski, and G. J. Iafrate, Handbook of Nanoscience, Engineering, and Technology, CRC Press LLC, , (2003).
- [12] F. Lindner, M. G. Schazel, H. Walther, A. Baltuska, E. Goulielmakis, F. Krausz, D. B. Milosevic, D. Bauer, W. Becker, and G. G. Paulus, Phys. Rev. Lett. **95**, 040401 (2005).
- [13] V. R. Almeida, C. A. Barrios, R. R. Panepucci, and M. Lipson Nature **431**, 1081 (2004).
- [14] M. A. Foster, A. C. Turner, J. E. Sharping, B. S. Schmidt, M. Lipson, and A. L. Gaeta, Nature **441**, 960 (2006).
- [15] J. E. Sharping, K. F. Lee, M. A. Foster, A. C. Turner, M. Lipson, A. L. Gaeta, and P. Kumar, to appear in Opt. Express , ().
- [16] X. Y. Zou, L. J. Wang, and L. Mandel, Opt. Commun. **84**, 351 (1991).
- [17] P. Kumar, M. Fiorentino, P. L. Voss, and J. E. Sharping, U. S. Patent No. 6,897,434 , (2005).
- [18] X. Li, C. Liang, K. F. Lee, J. Chen, P. L Voss, and P. Kumar, Phys. Rev. A **73**, 052301 (2006).
- [19] H. Takesue, and K. Inoue, Phys. Rev. A **70**, 031802 (2004).
- [20] Q. Lin, and Govind P. Agrawal, Opt. Lett. **31**, 3140 (2006).